

# Ground states of atomic Fermi gases in a two-dimensional optical lattice with and without population imbalance

Lin Sun<sup>1</sup> and Qijin Chen<sup>2,3,4,\*</sup>

<sup>1</sup>*Department of Physics and Zhejiang Institute of Modern Physics,  
Zhejiang University, Hangzhou, Zhejiang 310027, China*

<sup>2</sup>*Hefei National Research Center for Physical Sciences at the Microscale and School of Physical Sciences,  
University of Science and Technology of China, Hefei, Anhui 230026, China*

<sup>3</sup>*Shanghai Research Center for Quantum Science and CAS Center for Excellence in Quantum Information and Quantum Physics,  
University of Science and Technology of China, Shanghai 201315, China*

<sup>4</sup>*Hefei National Laboratory, University of Science and Technology of China, Hefei 230088, China*  
(Dated: May 10, 2022)

We study the ground state phase diagram of population balanced and imbalanced ultracold atomic Fermi gases with a short range attractive interaction throughout the crossover from BCS to Bose-Einstein condensation (BEC), in a two-dimensional optical lattice (2DOL) comprised of two lattice and one continuum dimensions. We find that the mixing of lattice and continuum dimensions, together with population imbalance, has an extraordinary effect on pairing and the superfluidity of atomic Fermi gases. In the balanced case, the superfluid ground state prevails the majority of the phase space. However, for relatively small lattice hopping integral  $t$  and large lattice constant  $d$ , a pair density wave (PDW) emerges unexpectedly at intermediate coupling strength, and the nature of the in-plane and overall pairing changes from particle-like to hole-like in the BCS and unitary regimes, associated with an abnormal increase in the Fermi volume with the pairing strength. In the imbalanced case, the stable polarized superfluid phase shrinks to only a small portion of the entire phase space spanned by  $t$ ,  $d$ , imbalance  $p$  and interaction strength  $U$ , mainly in the bosonic regime of low  $p$ , moderately strong pairing, and relatively large  $t$  and small  $d$ . Due to the Pauli exclusion between paired and excessive fermions within the confined momentum space, a PDW phase emerges and the overall pairing evolves from particle-like into hole-like, as the pairing strength grows stronger in the BEC regime. In both cases, the ground state property is largely governed by the Fermi surface topology. These findings are very different from the cases of pure 3D continuum, 3D lattice or 1DOL.

## I. INTRODUCTION

Ultracold Fermi gases provide an ideal platform for investigating the pairing and superfluid physics over the past decades, primarily owing to the high tunability of multiple parameters [1, 2]. Using a Feshbach resonance [3], one can tune the effective pairing strength from the weak coupling BCS limit all the way through to the strong pairing Bose-Einstein condensation (BEC) limit. There have been a great number of experimental and theoretical studies on ultracold Fermi gases in recent years, with many tunable parameters which have been made accessible experimentally, including pairing interaction strength [1], population imbalance [4–12], and dimensionality [13–15]. In particular, ultracold Fermi gases in an optical lattice exhibit rich physics due to the tunable geometry [16–18]. As is well known, population imbalance suppresses or destroys superfluidity in three-dimensional (3D) homogeneous systems [9, 19]. For example, superfluidity at zero temperature is completely destroyed at unitarity and in the BCS regime, whereas stable polarized superfluid (pSF) with a finite imbalance  $p$  exists only in the BEC regime [19]. Meanwhile, in the absence of population imbalance in a 3D lattice, one finds the superfluid transition temperature  $T_c \propto -t^2/U$  in the BEC regime, due to virtual pair unbinding in the pair hopping process [20, 21], which makes it hard to reach the superfluid phase in the BEC regime. (Here  $t$  is

the lattice hopping integral, and  $U < 0$  is the onsite attractive interaction). While the superfluid transition for both population balanced and imbalanced Fermi gases have been realized experimentally in the 3D continuum case (often in a trap), it has not been realized even for the balanced case in 3D lattices. However, superfluidity, long-range or Berezinskii-Kosterlitz-Thouless (BKT)-like [22], as well as pairing phenomena have been explored experimentally in 2D and 1D optical lattices [23–28] or quasi-2D traps [29–33]. Common to these experiments is the presence of one or two continuum dimensions. Until further breakthrough is made in cooling techniques, the presence of continuum dimensions seems to be crucial for the superfluid phase to be accessible experimentally so far in low dimensional optical lattices (and quasi-2D traps) besides the 3D continuum. We note, however, that these optical lattice experiments have mostly been restricted to the small  $t$  limit such that the coupling between different pancakes (2D planes) or cigar-shaped tubes (1D lines) is negligible. Therefore, a systematic investigation of the vast unexplored parameter space of the low dimensional optical lattices is important in order to uncover possible exotic and interesting new quantum phenomena.

In the presence of population imbalance, an open Fermi surface of Fermi gases in a one-dimensional optical lattice (1DOL), caused by large  $d$  and/or small  $t$ , often leads to destruction of the superfluid ground state in the BEC regime [34]. Our recent study on pairing and superfluidity of atomic Fermi gases in a two-dimensional optical lattice (2DOL), which is comprised of two lattice and one continuum dimen-

\* Corresponding author: qchen@uchicago.edu

sions, reveals that for relatively large  $d$  and small  $t$ , a pair density wave (PDW) ground state emerges in the regime of intermediate pairing strength, and the nature of the in-plane and overall pairing changes from particle-like to hole-like in the unitary and BCS regimes, with an unexpected nonmonotonic dependence of the chemical potential on the pairing strength [35].

In this paper, we focus on the ground state superfluid behavior of atomic Fermi gases in 2DOL, under the effects of lattice-continuum mixing, population imbalance and its interplay with the lattice parameters. We first investigate the evolution of the Fermi surface as a function of hopping integral  $t$  and lattice constant  $d$ , and then calculate the zero  $T$  superfluid phase diagram using the BCS-Leggett mean-field equations [36], but supplemented with various stability conditions, including those derived from finite-temperature formalism [9]. We explore the superfluid phase diagrams in various phase planes, as a function of lattice constant, hopping integral and interaction strength for population balanced cases and also of polarization for population imbalanced cases.

We find that in the population balanced case, while the phase diagram at zero  $T$  is dominated by the superfluid phase, a PDW ground state may emerge at intermediate pairing strength, for relatively small  $t$  and large  $d$ , and the nature of the in-plane and overall pairing changes from particle-like to hole-like in the BCS and unitary regimes. This is associated with an open Fermi surface, where the effective number density in the lattice dimensions can go above half filling. The PDW state originates from strong inter-pair repulsive interactions and relatively large pair size at intermediate pairing strength, which is also found in dipolar Fermi gases within the pairing fluctuation theory [37].

In the population imbalanced case, due to the constraint of various stability conditions, stable superfluid ground states are found to exist only in a small portion of the multi-dimensional phase space, spanned by the parameters  $t$ ,  $d$ ,  $p$  and  $U$ , mainly in the low  $p$  and bosonic regime of intermediate pairing strength, and for relatively large  $t$  and small  $d$ . As the pairing interaction becomes stronger in the BEC regime, the nature of the overall pairing of a polarized Fermi gas in 2DOL evolves from particle-like into hole-like. As manifested in the momentum distribution of the paired fermions and excessive majority fermions, there is a strong Pauli exclusion between them for small  $t$  and large  $d$ . Therefore, decreasing  $t$  and increasing  $d$  and  $p$  help to extend the hole-like pairing regime toward weaker coupling. These results are very different from their counterpart in pure 3D continuum, 3D lattices and 1DOL.

We mention that the values of  $t$  and  $d$  for which one finds hole-like pairing in the weaker coupling regime in the balanced case and in the stronger coupling regime in the imbalanced case do not overlap. This can be understood as the balanced case and the  $p \rightarrow 0^+$  case are not continuously connected at  $T = 0$ .

## II. THEORETICAL FORMALISM

### A. General theory

Here we consider a two-component ultracold Fermi gas with a short-range pairing interaction,  $V_{\mathbf{k},\mathbf{k}'} = U < 0$ , in 2DOL. The dispersion of noninteracting atoms without population imbalance is given by  $\xi_{\mathbf{k}} = \epsilon_{\mathbf{k}} - \mu \equiv k_z^2/2m + 2t[2 - \cos(k_x d) - \cos(k_y d)] - \mu$ , where  $k_z$  is the momentum in the  $z$  direction in the continuum dimension,  $k_x$  and  $k_y$  are the momenta in the lattice plane,  $t$  and  $d$  are the hopping integral and lattice constant in the  $xy$  plane, respectively, and  $\mu$  is the chemical potential. Following our recent works [15, 34, 38, 39], we take  $t$  to be physically accessible, under the constraint  $2mtd^2 < 1$  in our calculation. And the critical coupling for forming a two-body bound state of zero binding energy is given by  $U_c = -1/\sum_{\mathbf{k}} 1/2\epsilon_{\mathbf{k}} = -0.16072\sqrt{2m}/\sqrt{td^2}$ . Here and throughout we take the natural units and set  $\hbar = k_B = 1$ .

At zero temperature, the mean-field BCS-Leggett ground state follows the gap and number equations [36]

$$0 = \frac{1}{U} + \sum_{\mathbf{k}} \frac{1}{2E_{\mathbf{k}}}, \quad (1)$$

$$n = \sum_{\mathbf{k}} \left(1 - \frac{\xi_{\mathbf{k}}}{E_{\mathbf{k}}}\right), \quad (2)$$

where  $E_{\mathbf{k}} = \sqrt{\xi_{\mathbf{k}}^2 + \Delta^2}$  is the Bogoliubov quasiparticle dispersion, with an energy gap  $\Delta$ .

To make sure the mean-field solution is stable, we impose the requirement that the dispersion of the Cooper pairs be non-negative, both in the lattice plane and along the  $z$  direction. To this end, we extract the inverse pair mass (tensor) using the fluctuating pair propagator, as given in the pairing fluctuation theory which was previously developed for the pseudogap physics in the cuprates [40] and extended to address the BCS-BEC crossover in ultracold atomic Fermi gases [1]. In particular, we mention that, compared to rival  $T$ -matrix approximations for the pairing physics, the pair dispersion as extracted from this theory is gapless below  $T_c$ , fully compatible with the mean-field gap equation. Here the pairing  $T$  matrix is given by  $t_{\text{pg}}(Q) = U/[1 + U\chi(Q)]$ , with the pair susceptibility  $\chi(Q) = \sum_K G_0(Q - K)G(K)$ , the bare Green's function  $G_0(K) = (\omega - \xi_{\mathbf{k}})^{-1}$ , and the full Green's function  $G(K) = \frac{u_{\mathbf{k}}^2}{\omega - E_{\mathbf{k}}} + \frac{v_{\mathbf{k}}^2}{\omega + E_{\mathbf{k}}}$ , where  $u_{\mathbf{k}}^2 = (1 + \xi_{\mathbf{k}}/E_{\mathbf{k}})/2$  and  $v_{\mathbf{k}}^2 = (1 - \xi_{\mathbf{k}}/E_{\mathbf{k}})/2$  are the BCS coherence factors, and  $K \equiv (\omega, \mathbf{k})$ ,  $Q \equiv (\Omega, \mathbf{q})$  are four momenta.

The inverse  $T$ -matrix  $t_{\text{pg}}^{-1}(Q)$  can be expanded for small  $Q$ , given by  $t_{\text{pg}}^{-1}(\Omega, \mathbf{q}) \approx a_1\Omega^2 + a_0(\Omega - \Omega_{\mathbf{q}} + \mu_p)$ , with  $\Omega_{\mathbf{q}} = Bq_z^2 + 2t_B[2 - \cos(q_x d) - \cos(q_y d)]$ , and  $\mu_p = 0$  in the superfluid phase. Then we extract  $B = 1/2M$ , with  $M$  being the effective pair mass in the  $z$  direction, and  $t_B$  the effective pair hopping integral in the  $xy$  plane. The sign of  $a_0$  determines whether the fermion pairs are particle-like or hole-like, with positive  $a_0$  for particle-like pairing and negative  $a_0$  for hole-like pairing. For example, in a 3D lattice, in general one finds  $a_0 > 0$  for fermion density below half

filling,  $a_0 = 0$  at half filling due to particle-hole symmetry, and  $a_0 < 0$  above half filling. The sign of  $a_0$  is controlled by the average of the inverse band mass [41]. While one could perform a particle-hole transformation for a pure lattice case, it does not seem to be feasible in our case since both lattice and continuum dimensions are present. The expressions for the coefficients  $a_1$ ,  $a_0$ ,  $B$  and  $t_B$  can be readily derived during the Taylor expansion. In this way, using the solution for  $(\mu, \Delta)$  from Eqs. (1)-(2), we can extract the pair dispersion  $\tilde{\Omega}_{\mathbf{q}} = (\sqrt{a_0^2 + 4a_1a_0\Omega_{\mathbf{q}}} - a_0)/2a_1$ . The non-negativeness of the pair dispersion implies that the pairing correlation length (squared)  $\xi^2 = a_0B$  and  $\xi_{xy}^2 = a_0t_Bd^2$  must be positive.

For the population imbalanced case, the spin polarization is defined via  $p = (n_{\uparrow} - n_{\downarrow})/(n_{\uparrow} + n_{\downarrow})$ , where spin index  $\sigma = \uparrow, \downarrow$  refers to the majority and minority components, respectively. Then the dispersion of noninteracting atoms is modified as  $\xi_{\mathbf{k}\sigma} = \epsilon_{\mathbf{k}} - \mu_{\sigma}$ , with  $\mu_{\sigma}$  the chemical potential for spin  $\sigma$ .

Now the bare and full Green's functions are given by

$$G_{0\sigma}(K) = \frac{1}{\omega - \xi_{\mathbf{k}\sigma}}, \quad \text{and}$$

$$G_{\sigma}(K) = \frac{u_{\mathbf{k}}^2}{\omega - E_{\mathbf{k}\sigma}} + \frac{v_{\mathbf{k}}^2}{\omega + E_{\mathbf{k}\bar{\sigma}}},$$

respectively, where  $\bar{\sigma}$  is the opposite spin of  $\sigma$ ,  $E_{\mathbf{k}\uparrow} = E_{\mathbf{k}} - h$ , and  $E_{\mathbf{k}\downarrow} = E_{\mathbf{k}} + h$ , with  $\mu = (\mu_{\uparrow} + \mu_{\downarrow})/2$ , and  $h = (\mu_{\uparrow} - \mu_{\downarrow})/2$ . Thus  $E_{\mathbf{k}\uparrow}$  becomes gapless, as it should, in order to accommodate the excessive majority fermions [See Eq. (5) below]. These gapless fermions will contribute in both the gap and number equations.

Following the BCS self-consistency condition and the number constraint, we arrive at the gap and number equations at zero  $T$  in the presence of population imbalance:

$$0 = \frac{1}{U} + \sum_{\mathbf{k}} \frac{\Theta(E_{\mathbf{k}\uparrow})}{2E_{\mathbf{k}}}, \quad (3)$$

$$n = \sum_{\mathbf{k}} \left[ \left(1 - \frac{\xi_{\mathbf{k}}}{E_{\mathbf{k}}}\right) + \Theta(-E_{\mathbf{k}\uparrow}) \frac{\xi_{\mathbf{k}}}{E_{\mathbf{k}}} \right], \quad (4)$$

$$pn = \sum_{\mathbf{k}} \Theta(-E_{\mathbf{k}\uparrow}), \quad (5)$$

where  $\Theta(x)$  is the Heaviside step function, and  $n = n_{\uparrow} + n_{\downarrow}$  and  $\delta n = n_{\uparrow} - n_{\downarrow} = pn$  are the total and the difference of fermion densities, respectively.

In the imbalanced case, the pair susceptibility is modified as  $\chi(Q) = \sum_{K,\sigma} G_{0\sigma}(Q-K)G_{\bar{\sigma}}(K)/2$ , which is consistent with the BCS self-consistency condition so that the pair dispersion remains gapless at  $q = 0$ . Then we follow the same procedure as in the balanced case, and extract the inverse pair mass tensor along with coefficients  $a_0$  and  $a_1$  via the Taylor expansion of the inverse  $T$  matrix,  $t_{\text{pg}}^{-1}(Q)$ .

Equations (3)-(5) form a closed set of self-consistent equations, and can be used to solve for  $(\mu, h, \Delta)$  as a function of  $(U, t, d, p)$ , which is then further constrained by various stability conditions.

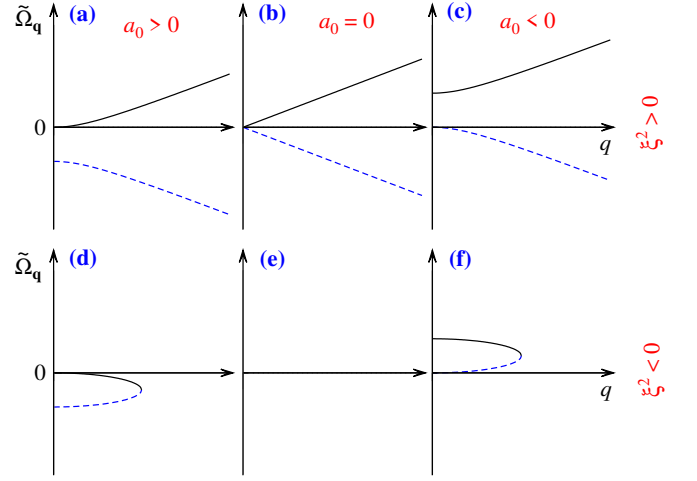


Figure 1. Qualitative behavior of the pair dispersion  $\tilde{\Omega}_{\mathbf{q}}$  for different signs of  $a_0$  and  $\xi^2$ . For illustration purpose, a simple isotropic quadratic  $\Omega_{\mathbf{q}} = \xi^2 q^2/a_0$  is used. The three columns are for  $a_0 > 0$ ,  $a_0 = 0$  and  $a_0 < 0$  from left to right, and the top and bottom rows are  $\xi^2 > 0$  and  $\xi^2 < 0$ , respectively. The black solid curves in the top row represent propagating modes.

## B. Stability analysis

As shown in the 3D continuum and 1DOL cases, in the presence of population imbalance, not all solutions of Eqs. (3)-(5) are stable [9, 19, 42].

Following the stability analysis of Refs. [9, 19], the stability condition for the superfluid phase requires that for fixed  $\mu$  and  $h$ , the solution for the excitation gap  $\Delta$  is a minimum of the thermodynamic potential  $\Omega_S$ , which is demonstrated to be equivalent to the positive definiteness of the generalized compressibility matrix [9, 43]. Thus we have

$$\frac{\partial^2 \Omega_S}{\partial \Delta^2} = \sum_{\mathbf{k}} \frac{\Delta^2}{E_{\mathbf{k}}^2} \left[ \frac{\Theta(E_{\mathbf{k}\uparrow})}{E_{\mathbf{k}}} - \delta(E_{\mathbf{k}\uparrow}) \right] > 0, \quad (6)$$

where  $\delta(x)$  is the delta function.

In addition, the positivity of the pair dispersion in the entire momentum space imposes another strong stability condition. Illustrated in Fig. 1 are the qualitative behaviors of the pair dispersion, for different signs of  $a_0$  and  $\xi^2$ . For illustration purpose, a simple isotropic quadratic dispersion is assumed. In general, there are two branches of the dispersion, from the inverse  $T$ -matrix expansion up to the  $\Omega^2$  order. The positive branch represents a propagating mode, while the negative branch represents a hole-like mode which contributes to quantum fluctuations. The case of  $a_0 > 0$  and  $\xi^2 > 0$  (Fig. 1(a)) corresponds to particle-like pairing, with a monotonically increasing energy and a positive effective pair mass,  $B > 0$  and  $t_B > 0$ , so that  $q = 0$  is the bottom of the pair energy. For the  $a_0 < 0$  case (Fig. 1(c)), this dispersion flips upside down into the blue-dashed hole mode. This corresponds to hole-like pairing, for which  $q = 0$  becomes a local maximum, with  $B < 0$  and  $t_B < 0$ , similar to the hole band in a semiconductor. In case of a pure lattice, one could flip the

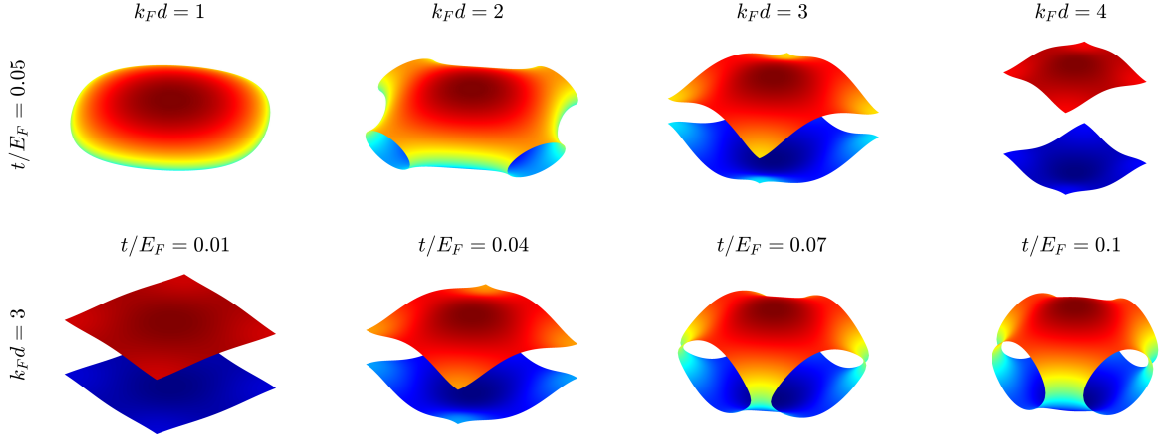


Figure 2. Evolution of the Fermi surface of atomic Fermi gases in 2DOL, for fixed  $t/E_F = 0.05$  (top row) with  $k_F d = 1, 2, 3$  and  $4$ , and fixed  $k_F d = 3$  (bottom row) with  $t/E_F = 0.01, 0.04, 0.07$  and  $0.1$ , from left to right.

sign of  $a_0$  via a particle-hole transformation so that this blue-dashed line is flipped back to become positive as the dispersion for hole pairs. However, for our present case, due to the presence of the continuum dimension, there is no easy way to do a particle-hole transformation so that we have to stay with the (black solid) gapped positive branch, which is a flip of the hole branch in Fig. 1(a), as the dispersion of particle-like Cooper pairs. When  $a_0 = 0$ , the two branches become symmetric, without a gap. For all three cases, the coefficients of the  $q^2$  terms in the inverse  $T$  matrix expansion,  $\xi^2$  and  $\xi_{xy}^2$ , must be positive. (Note that  $a_1$  is always positive.) Indeed, as shown in Figs. 1(d-f), for a negative  $\xi^2$ , the dispersion  $\tilde{\Omega}_q$  of both particle-like (Figs. 1(d)) and hole-like (Figs. 1(f)) pairs quickly become diffusive and thus cease to exist, unless higher order terms, e.g., the  $q^4$  terms, are included. In that case, the pair dispersion will reach a minimum at a non-zero  $q$ . Our numerics shows that in 2DOL,  $\xi^2$  in the continuum dimension remains positive in general but  $\xi_{xy}^2 \propto a_0 t_B$  in the lattice plane may indeed change sign so that  $\xi_{xy}^2 > 0$  will constitute another stability requirement for the superfluid phase.

Finally, the superfluid density must also be positive definite in a stable superfluid. This, however, has been found to be a relatively weaker constraint in the cases of 3D continuum [9, 19].

### C. Superfluid density

As a representative transport property, superfluid density is an important quantity in the superfluid phase. While it is always given by  $n/m$  at zero  $T$  for the balanced case in 3D continuum, it will take the average of the inverse band mass in the presence of a lattice. Furthermore, in the presence of population imbalance, it may become negative [9, 19, 44], signaling an instability of the superfluid state. Here we shall also investigate the behavior of the anisotropic superfluid density ( $n_s/m$ ), and pay close attention to the population imbalanced case and the situations where it becomes negative.

The expression for superfluid density can be derived using

the linear response theory. Following Refs. [9, 19, 40, 44, 45], we obtain for zero  $T$

$$\left(\frac{n_s}{m}\right)_i = \sum_{\mathbf{k}} \frac{\Delta_{\text{sc}}^2}{E_{\mathbf{k}}^2} \left[ \frac{\Theta(E_{\mathbf{k}\uparrow})}{E_{\mathbf{k}}} - \delta(E_{\mathbf{k}\uparrow}) \right] \left( \frac{\partial \xi_{\mathbf{k}}}{\partial k_i} \right)^2, \quad (7)$$

where  $i = x, y$  and  $z$  for the lattice and the continuum directions, respectively.

## III. NUMERICAL RESULTS AND DISCUSSIONS

Due to the multiple tunable parameters for the present 2DOL, the complete multidimensional phase diagram can be extremely complex. Therefore, we shall focus on the lattice effect for the  $p = 0$  case, together with the population imbalance for the  $p \neq 0$  case, to give several representative and informative phase diagrams. For our numerics, it is convenient to define Fermi momentum  $k_F = (3\pi^2 n)^{1/3}$  and Fermi energy  $E_F \equiv k_B T_F = \hbar^2 k_F^2 / 2m$ , as the units of momentum and energy, respectively, which also sets  $2m = 1$ . Note, however, that this  $E_F$  is *not* equal to the chemical potential in the noninteracting limit.

### A. Fermi surfaces in the noninteracting limit

Fermi surface plays an important role in the superfluid and pairing behavior of atomic Fermi gases. For 2DOL, it is very different from the 3D continuum or 3D lattice case, so is it from 1DOL [15, 34, 38]. This will lead to different physics. Here we first present the shape and topology of the Fermi surface for a series of representative sets of lattice parameters ( $t, d$ ). Shown in Fig. 2 is the typical evolution behavior of the Fermi surface, calculated self-consistently in the noninteracting limit at zero temperature. The top row shows the evolution with the lattice constant, for  $k_F d = 1, 2, 3$  and  $4$  at fixed hopping integral  $t/E_F = 0.05$ . Then the bottom row shows the effect of hopping integral, with  $t/E_F = 0.01, 0.04, 0.07$ , and  $0.1$  and fixed  $k_F d = 3$ .

The lattice constant  $d$  provides a confinement in the momentum space; the larger  $d$  the stronger confinement. The top row in Fig. 2 suggests that the Fermi surface becomes thicker along the  $z$  direction as  $d$  increases for fixed  $t$ . Indeed, fermions feel a stronger confinement in the lattice dimensions with a shrinking first Brillouin zone (BZ), as  $k_F d$  increases from 1 to 4, and thus need to occupy higher  $k_z$  states to keep the Fermi volume unchanged, so that the noninteracting fermionic chemical potential is pushed up. As a rough estimate, the maximum occupied  $k_z$  increases by a factor of 16 from left to right. For relatively small  $t/E_F = 0.05$ , the shape and topology of the Fermi surface evolve from a closed plate for  $k_F d = 1$  into one with only the top and bottom faces while completely open on the four sides at the BZ boundary of the lattice dimensions for  $k_F d = 3$  and 4. For the intermediate  $k_F d = 2$ , the Fermi surface is open only at the center of the four side faces at the BZ boundary. At the same time, the effective filling factor in the lattice dimensions increases to nearly unity as  $k_F d$  increases from 1 to 4. In this way, for large  $d$ , fermion dispersion on the Fermi surface on average becomes hole-like in the lattice plane, while it always remains particle-like in the continuum dimension.

On the other hand, a smaller  $t$  makes the fermion energy less dispersive in the lattice dimensions, and thus the lattice band becomes narrower and more fully filled. In other words, fermions will tend not to go to higher  $k_z$  states until the BZ at lower  $k_z$  is fully occupied, leading to a flatter top and bottom of the Fermi surface. This will also pull down the noninteracting fermionic chemical potential. As shown in the bottom row in Fig. 2, the Fermi surface becomes thinner and flatter in the  $z$  direction as  $t/E_F$  decreases from 0.1 to 0.01 for fixed  $k_F d = 3$ . In contrast, the  $t/E_F = 0.07$  and 0.1 cases have a much more dispersive Fermi surface as a function of the in-plane momentum  $(k_x, k_y)$ . Fermions at high  $(k_x, k_y)$  states are removed for relatively large hopping integral  $t/E_F = 0.07$  and 0.1.

The evolution of the Fermi surface reveals that the in-plane fermion motion on the Fermi surface becomes hole-like for relatively small  $t$  and large  $d$ . As a result, the nature of the in-plane and overall pairing in this case will also change from particle-like to hole-like when the contributions from lattice dimensions are dominant in the BCS and unitary regimes [35].

It should be mentioned that in the strong pairing regime, the detailed shape of the Fermi surface is no longer relevant, as pairing extends essentially to the entire momentum space. However, the confinement in the momentum space imposed by the lattice periodicity is always present and will govern the physical behavior in the BEC regime.

### B. Phase diagram for the population balanced case

It is known from the 3D continuum case that the balanced case and the imbalanced case with  $p \rightarrow 0^+$  are not continuously connected in the BCS and unitary regimes at  $T = 0$  [19, 46]. Population imbalance leads to very distinct behaviors. Therefore, we present in this section the balanced results only.

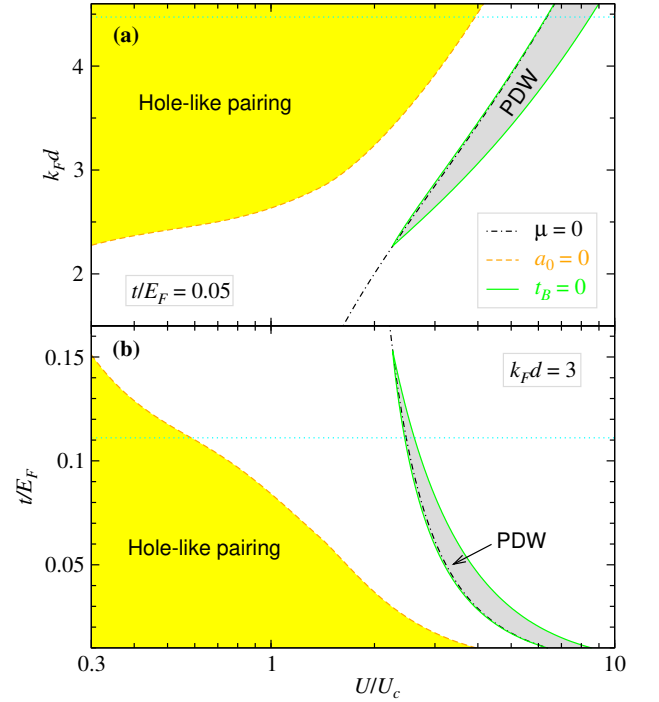


Figure 3. Phase diagram in the balanced case in the (a)  $d - U$  plane for  $t/E_F = 0.05$  and (b) in the  $t - U$  plane for  $k_F d = 3$ . The (orange dashed)  $a_0 = 0$  curve separates hole-like pairing (yellow shaded region) on the left from particle-like pairing on the right. Enclosed inside the (green)  $t_B = 0$  line is a PDW ground state (grey shaded region). Also plotted is the (black dot-dashed)  $\mu = 0$  line. The (cyan) dotted line denotes the upper limit for (a)  $d$  and (b)  $t$ , respectively, as defined by  $2mtd^2 \leq 1$ .

In Fig. 3, we present a typical phase diagram (a) in the  $d - U$  plane, for fixed relatively small  $t/E_F = 0.05$ , and (b) in the  $t - U$  plane, for relatively large  $k_F d = 3$ , corresponding to the cases of the top and bottom rows in Fig. 2, respectively. The lattice constant in panel (a) ranges from relatively small  $k_F d = 1$  with  $2mtd^2 = 0.05$  to the upper limit  $k_F d = 2\sqrt{5}$  with  $2mtd^2 = 1$  denoted by the horizontal (cyan) dotted line, and the hopping integral in panel (b) ranges from relatively small  $t/E_F = 0.01$  with  $2mtd^2 = 0.09$  to the upper limit  $t/E_F = 1/9$  with  $2mtd^2 = 1$  denoted by the horizontal (cyan) dotted line. In either panel, the (black dot-dashed)  $\mu = 0$  curve defines the boundary between the fermionic and the bosonic regimes. The (yellow) shaded region on the left of the (orange) dashed  $a_0 = 0$  curve is a hole-like pairing regime with  $a_0 < 0$ , whereas the overall pairing evolves from hole-like into particle-like with  $a_0 > 0$  across the  $a_0 = 0$  curve. A PDW ground state with  $t_B < 0$  emerges within the grey shaded region, enclosed within the (green)  $t_B = 0$  curve. The entire phase space is a superfluid except for the PDW phase. Note that the PDW phase usually starts immediately before  $\mu$  decreases down to zero, as the pairing strength increases. The fact that there are two branches of the  $t_B = 0$  curve indicates that there is a reentrant behavior of  $T_c$  as a function of pairing strength. In the absence of population imbalance, similar reentrant behavior of superfluidity and associated PDW



ground state have *not* been found in any other balanced systems with a short range pairing interaction, except in a very narrow range of density slightly above 0.53 in the attractive Hubbard model [45, 47, 48]. With a long-range anisotropic dipole-dipole interaction, however, such a reentrant behavior and PDW state have been predicted in the  $p$ -wave superfluid in dipolar Fermi gases [37].

As shown in Fig. 3, the interaction range for hole-like pairing extends toward stronger pairing regime with (a) increasing  $d$  or (b) decreasing  $t$ . This can be explained by the evolution of the shape and topology of the Fermi surface, as shown in Fig. 2. As  $d$  increases or  $t$  decreases, the Fermi surface gradually opens up at the four  $X$  or  $Y$  points located at  $(k_x, k_y) = (\pm\pi/d, 0)$  and  $(0, \pm\pi/d)$ , and becomes fully open at the first BZ boundary for large  $d$  small  $t$ , leading to an effective filling factor above  $1/2$  in the lattice dimensions. In contrast to the 1DOL case, the existence of two lattice dimensions is enough to dominate the contributions of the remaining one continuum dimension (which is always particle-like due to its parabolic fermion dispersion), so that both the in-plane and the overall pairing becomes hole-like when  $d$  is large or  $t$  is small, with  $a_0 < 0$  in the linear frequency term of the inverse  $T$  matrix expansion. This is especially true in the weak coupling regime, where the superfluidity is more sensitive to the underlying Fermi surface. As the interaction goes stronger toward the BEC regime, the gap becomes large and the Fermi level (i.e., chemical potential  $\mu$ ) decreases and then becomes negative, hence the shape of the non-interacting Fermi surface is no longer important. In this case, the contributions from the lattice dimensions will spread evenly across the entire BZ, so that the continuum dimension will become dominant, and the overall pairing eventually changes from hole-like to particle-like (with  $a_0 > 0$ ). As shown in Fig. 2, within the occupied range of  $k_z$ , the average (or effective) filling factor within the first BZ in the  $xy$  plane increases with increasing  $d$  and/or decreasing  $t$ . Therefore, as  $d$  increases, or  $t$  decreases, the effect of the above-half-filling status persists into stronger pairing regime, and thus the hole-like pairing region in Fig. 3 extends toward right.

Shown in Fig. 4 is the behavior of (a)  $\mu$  as a function of  $U$ , along with (b)  $2n_p/n$ , where  $n_p \equiv a_0\Delta^2$ , for  $t/E_F = 0.05$  and  $k_F d = 3$ . Also plotted are  $a_0$  and  $\Delta$ . This corresponds to a horizontal cut at  $k_F d = 3$  in Fig. 3(a) or at  $t/E_F = 0.05$  in Fig. 3(b). Inside the hole-like pairing regime,  $a_0 < 0$  and thus the chemical potential  $\mu$  goes above its noninteracting value. This can be seen from the expression [35, 45]

$$\sum_{\mathbf{k}} \Theta(-\xi_{\mathbf{k}}) = n/2 - a_0\Delta^2. \quad (8)$$

The chemical potential  $\mu$  increases with the pairing strength, until it reaches a maximum where  $n_p$  reaches a minimum. Here  $2n_p/n$  is roughly the pair fraction, which reaches unity in the BEC regime. This plot is very close to its counterpart at  $T_c$ , which can be found in Ref. [35], since the temperature dependencies of both  $\mu$  and  $a_0$  are weak, except that here  $a_0$  changes sign at a slightly larger  $U/U_c$ . As usual, the excitation gap  $\Delta$  increases with  $U/U_c$ .

The PDW ground state in Fig. 3 with  $t_B < 0$  at a interme-

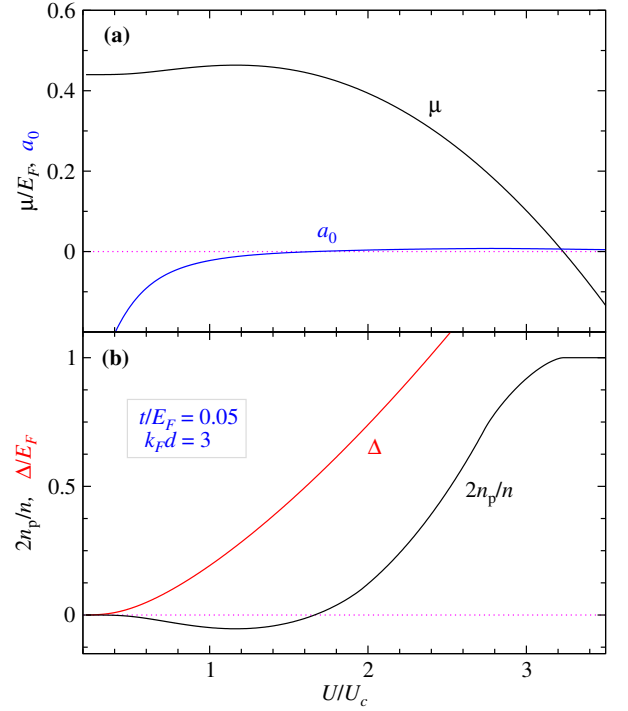


Figure 4. Behaviors of (a)  $\mu$  and  $a_0$  and (b)  $2n_p/n$  and  $\Delta$  as a function of  $U/U_c$  for  $t/E_F = 0.05$  and  $k_F d = 3$  without population imbalance. The maximum of  $\mu$  corresponds to the minimum of  $2n_p/n$ .

diating coupling strength for (a) relatively large  $k_F d$  with fixed  $t/E_F = 0.05$  or (b) small  $t$  with fixed  $k_F d = 3$  is associated with the strong inter-pair repulsive interaction, relatively large pair size and high pair density. Close to  $\mu = 0$ , nearly all fermions have paired up with a relatively large pair size and a heavy effective pair mass, and the inter-pair repulsive interaction becomes strong. A large  $d$  or small  $t$  strongly suppresses the pairing hopping kinetic energy, and the large pair size and high pair density strongly reduce the pair mobility. All these factors lead to Wigner crystallization and hence PDW in the  $xy$  plane, which can also be called a Cooper pair insulator. The negative sign of  $t_B$  within the grey shaded region indicates that the minimum of the pair dispersion  $\tilde{\Omega}_{\mathbf{q}}$  has shifted from  $\mathbf{q} = 0$  to  $\mathbf{q} = (\pi/d, \pi/d, 0)$ , with crystallization wave vector  $(q_x, q_y)$  in the  $xy$  plane. As the pairing interaction increases in the BEC regimes, the pair size shrinks and inter-pair repulsive interaction becomes weak; hence  $t_B$  changes from negative back to positive, corresponding to a quantum phase transition from a PDW insulator to a superfluid.

Combining Figs. 2 and 3, we find that the emergence of hole-like pairing and the PDW phase is associated with the open Fermi surface topology. Once the Fermi surface is closed, both hole-like pairing and the PDW phase disappear.

In case of a closed Fermi surface, typical behaviors of the chemical potential  $\mu$  and the excitation gap  $\Delta$  for the balanced case can be seen from the  $p = 0$  lines in Fig. 5, calculated for  $t/E_F = 0.05$  and  $k_F d = 1$ . Here  $\mu$  decreases monotonically with  $U/U_c$ . Without a hole-like pairing regime, these solutions look qualitatively similar to other cases, e.g., in 3D

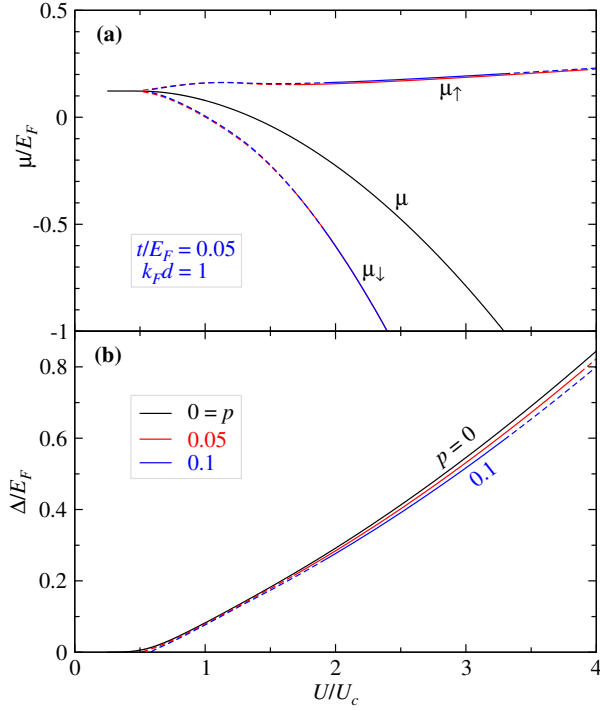


Figure 5. Behaviors of (a)  $\mu$  or  $\mu_\sigma$  and (b)  $\Delta$  as a function of  $U/U_c$  for  $p = 0$  (black), 0.05 (red) and 0.1 (blue lines), with fixed  $t/E_F = 0.05$  and  $k_F d = 1$ . Here solid and dashed lines denote stable and unstable solutions, respectively.

continuum or 3D lattice, except that they follow a different asymptotic behavior in the BEC limit [35].

### C. Phase diagram for the population imbalanced case

We now proceed and present our results for the population imbalanced case. With the added parameter  $p$ , the phase diagram becomes much more complicated. It renders the otherwise superfluid state unstable in the vast areas in the phase space.

To make the comparison easier, we begin by presenting phase diagrams in Fig. 6 in the same (a)  $d - U$  and  $t - U$  planes, as in Fig. 3, but with a tiny nonzero  $p = 0.001$ . Here a normal gas phase (grey shaded) emerges in the weak coupling regime, delineated by the (black solid)  $T_c^{\text{MF}} = 0$  line, which is given by Eqs. (3)-(5) with  $\Delta = 0$ . Indeed, in the presence of an imbalance, pairing cannot take place for an arbitrarily weak interaction. There exists a stable pSF phase (yellow shaded), defined by the (green solid)  $t_B = 0$  line and further confined by the stability condition (red solid line). The pSF phase resides in the low  $d$  and large  $t$  regime. A PDW ground state emerges in the dot shaded region, enclosed by the  $t_B = 0$  line and the dashed part of the (red) stability line. Then the rest unshaded space allows for an unstable mean-field superfluid solution, which may yield to phase separation. Now that the underlying lattice in the  $xy$  plane breaks the continuous translational symmetry, the exotic Fulde-Ferrell-Larkin-

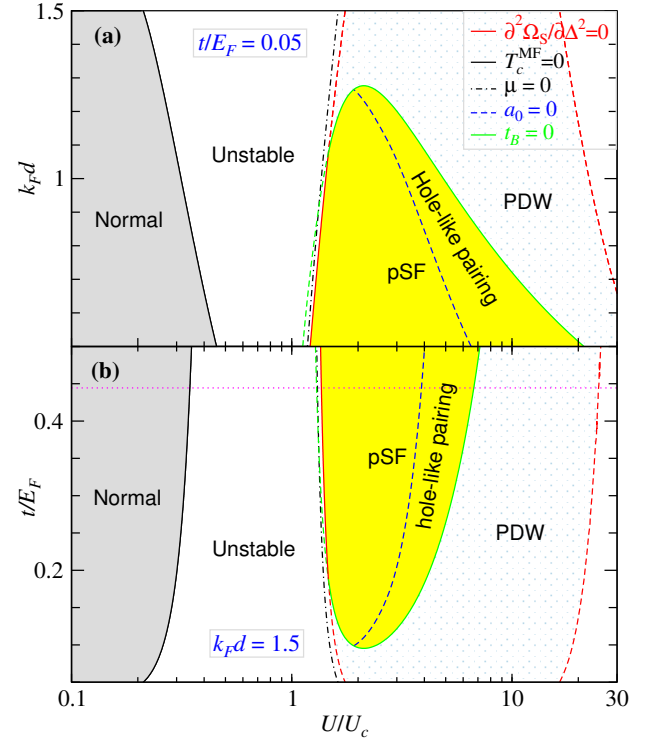


Figure 6. Phase diagrams at  $p = 0.001$  in the (a)  $d - U$  plane with  $t/E_F = 0.05$  and in the (b)  $t - U$  plane with  $k_F d = 1.5$ , respectively. As labeled, the solid lines along with the (red) stability line split the diagram into four phases: Normal gas (grey shaded, on the left of the black  $T_c^{\text{MF}} = 0$  line), unstable mean-field superfluid (unshaded), PDW phase (dot shaded), and stable polarized superfluid (yellow shaded region, bounded by the green  $t_B = 0$  line). Pairing on the right of the  $a_0 = 0$  line (blue dashed) has a hole-like nature. The chemical potential  $\mu = 0$  line (black dot-dashed) separates the fermionic regime (one the left) from the bosonic regime (on the right). The (magenta) dotted line sets the upper bound for  $t$  via  $2mtd^2 \leq 1$ .

Ovchinnikov (FFLO) states may possibly exist in part of the unstable region [49–51].

One can immediately tell that the vertical axes in Fig. 6 take different parameter ranges from those in Fig. 3, even though the imbalance  $p = 0.001$  is very small. While the  $d - U$  phase diagram in Fig. 6(a) is still calculated with  $t/E_F = 0.05$ , the stable pSF phase is now restricted to relatively small  $d$  (yellow shaded area). However, the  $t - U$  phase diagram has to be calculated at a much smaller  $d$ , with  $k_F d = 1.5$ , as there is no stable pSF phase for  $k_F d = 3$  within the constraint  $2mtd^2 \leq 1$  (i.e.,  $t/E_F \leq 1/9$ ). In both cases in Fig. 6, the Fermi surface is closed. Unlike the balanced cases, one cannot find a stable superfluid solution with an open Fermi surface. For this reason, one does not find a hole-like pairing region in the weak coupling regime, but rather one in the strong coupling regime, on the right of the (blue dashed)  $a_0 = 0$  line. Note that in the superfluid phase of hole-like pairing (on the right of the blue dashed line), both  $a_0$  and  $t_B$  are negative but the product  $\xi_{xy}^2$  is positive. Outside the  $t_B = 0$  curve, we have  $\xi_{xy}^2 < 0$ , so that the mean-field superfluid solution becomes unstable,

yielding to the PDW phase. The smallness of  $p$  suggests that the ground state of  $p \rightarrow 0^+$  is *not* continuously connected to the  $p = 0$  case, consistent with that in 3D continuum [19]. In comparison with Fig. 3, the current large PDW phase in the bosonic regime is totally a consequence of population imbalance.

Now we take  $p$  as a varying parameter and explore phase diagrams in the  $p - U$  plane. Shown in Fig. 7 are the phase diagrams for (a)  $(t/E_F, k_F d) = (0.15, 1)$ , (b)  $(0.05, 1)$ , and (c)  $(0.15, 1.5)$ . Panels (b) and (c) show the effect of changing  $t$  and  $d$ , respectively. In all three cases, there are three different phases, delineated by solid lines, as well as a PDW phase. A normal gas phase (grey shaded) takes the weaker coupling and larger  $p$  area, on the left of the  $T_c^{\text{MF}} = 0$  curve. The vast majority is an unstable mean-field superfluid (unshaded), which should yield to phase separation or FFLO solutions. The stable pSF phase (yellow shaded) occupies only a small area. Finally, the PDW phase (dot shaded) takes the small region next to the pSF phase, bounded by the (red dashed) stability  $\partial^2 \Omega_S / \partial \Delta^2 = 0$  line and (green solid)  $t_B = 0$  line. When compared with panel (a), one readily sees that the pSF phase shrinks as  $t$  decreases (panel (b)) and/or as  $d$  increases (panel (c)). This is because both increasing  $d$  and reducing  $t$  lead to stronger momentum confinement in the lattice dimensions. In agreement with Fig. 6, the Fermi surface for all these three cases are closed. Note that the (red) stability line and the (green)  $t_B = 0$  line cross into each other, and the pSF phase is bounded by the stronger of these two conditions. Here also plotted are the lines along which the superfluid density vanishes. As found in 3D continuum, the positivity of superfluid density constitutes a much weaker stability constraint, as both lines of  $(n_s/m)_x = 0$  in the lattice dimension and of  $(n_s/m)_z = 0$  in the continuum dimension lie completely within the unstable area. Note that while the  $(n_s/m)_z = 0$  line looks very similar to its 3D continuum counterpart, the  $(n_s/m)_x = 0$  line exhibits an unusual nonmonotonic behavior, caused by the lattice effect. From the (violet dotted)  $\mu = 0$  curve, one readily sees that, as in Fig. 6, the pSF phase resides completely within the bosonic regime.

The fact that the pSF phase exists only in a small bosonic region (in both Fig. 6 and Fig. 7) is in stark contrast with the 3D continuum case, for which the stability line  $\partial^2 \Omega_S / \partial \Delta^2 = 0$  extends monotonically up to  $p = 1$ , and a polarized superfluid exists for arbitrary imbalance  $p$  in the BEC regime [19]. Apparently, this difference can be attributed to the presence of two lattice dimensions. Indeed, for 1DOL, with only one lattice dimension, the stability line already cannot extend to  $p = 1$ . However, the pSF phase in 1DOL can extend all the way to the deep BEC limit [42]. This is also supported by the fact that with three lattice dimensions in a 3D attractive Hubbard model, one can barely find a pSF state except at very low density and extremely low  $p$  [52]. Therefore, one can conclude that more lattice dimensions make it more difficult to have a stable pSF ground state.

This phenomena can be easily understood from the momentum distribution of paired fermions, which would be given by  $v_k^2$  had there been no imbalance. In 3D continuum,  $v_k^2$  in the deep BEC regime extends to the entire infinitely large

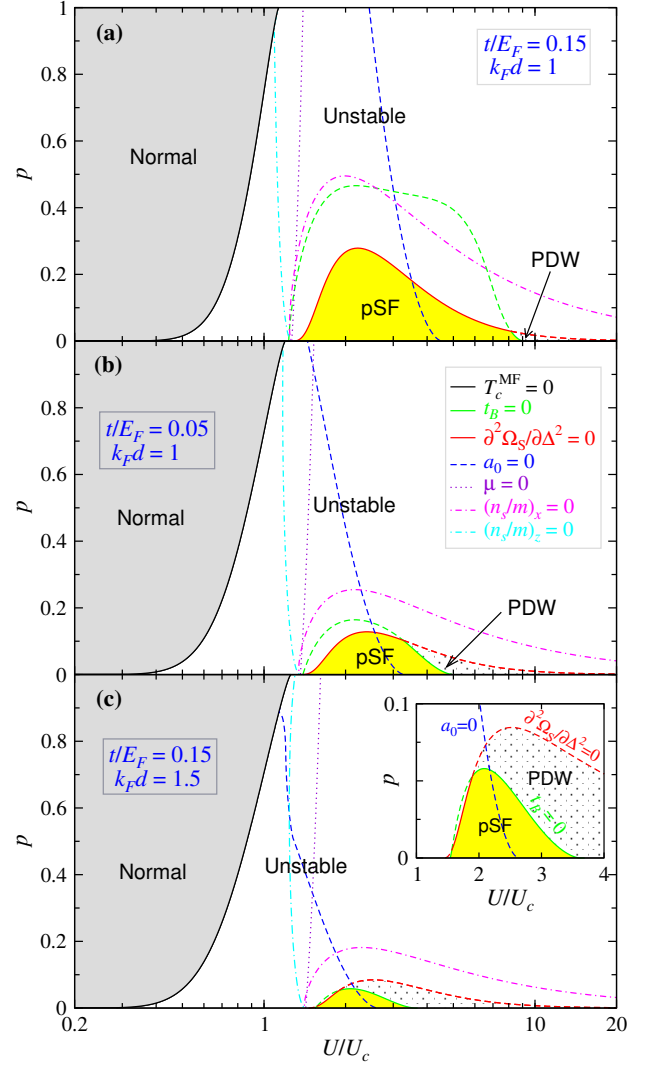


Figure 7. Phase diagrams in the  $p - U$  plane for (a)  $(t/E_F, k_F d) = (0.15, 1)$ , (b)  $(0.05, 1)$ , and (c)  $(0.15, 1.5)$ . The solid  $T_c^{\text{MF}} = 0$  (black) and  $t_B = 0$  (green) lines, as well as the (red) stability  $\partial^2 \Omega_S / \partial \Delta^2 = 0$  line (both solid and dashed) divide the plane into four phases: Normal gas (grey shaded), unstable superfluid (unshaded), PDW phase (dot shaded), and stable pSF phase. Across the  $a_0 = 0$  line (blue dashed) the pairing nature changes from particle-like (on the left) to hole-like (on the right). The  $\mu = 0$  line (violet dotted) separate fermionic (left) from bosonic (right) regimes. Also plotted are lines of the superfluid density  $(n_s/m)_x = 0$  (magenta dot-dashed) in the  $x$  direction, and  $(n_s/m)_z = 0$  (cyan dot-dashed) in the  $z$  direction. Superfluid density is negative on the weaker coupling or larger  $p$  side of these curves. Shown in the inset of panel (c) is a zoom-in of the pSF phase.

momentum space in all directions, leading to a vanishingly small occupation for paired fermions. Therefore, the excessive majority fermions can readily occupy the low momentum states, with essentially no Pauli blocking from paired fermions. However, when one or more lattice dimensions are present, the momentum in these dimensions is restricted to the first BZ, so that  $v_k^2$  in these dimensions cannot be infinitesimally



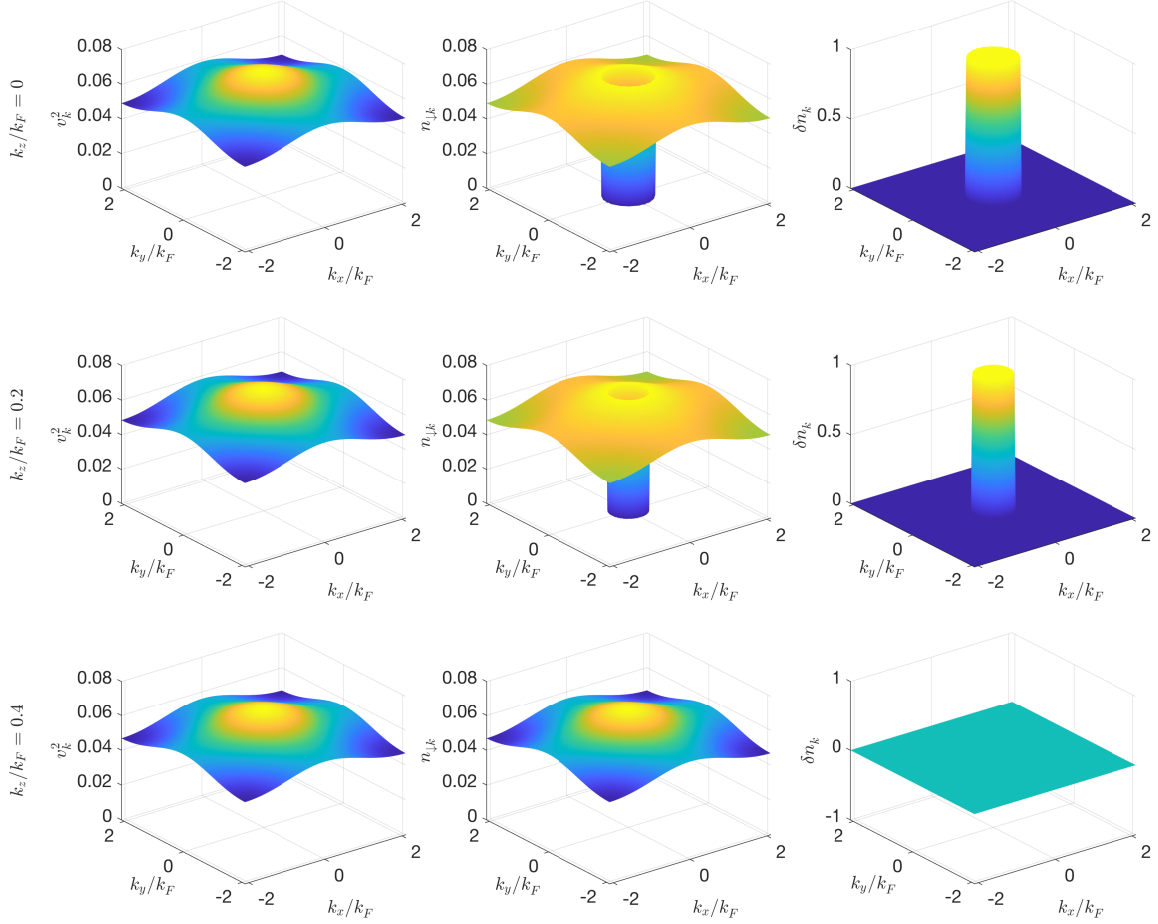


Figure 8. Momentum distributions of  $v_{\mathbf{k}}^2$  (left),  $n_{\mathbf{k}\downarrow}$  (middle) and  $\delta n_{\mathbf{k}}$  (right column) in the  $(k_x, k_y)$  plane at different  $k_z/k_F = 0$  (top), 0.2 (middle) and 0.4 (bottom row), with  $U/U_c = 4$  and  $p = 0.05$ , for  $t/E_F = 0.15$  and  $k_F d = 1.5$ . The excessive fermion distribution,  $\delta n_{\mathbf{k}}$ , occupies the low in-plane momentum part and below  $k_z/k_F = 0.4$  (right column),  $v_{\mathbf{k}}^2$  (left column) remains roughly constant in the entire BZ and for  $|k_z/k_F| \leq 0.4$ , and  $n_{\mathbf{k}\downarrow}$  (middle column) is given by  $v_{\mathbf{k}}^2$  but with the central part expelled.

mally small even in the extreme BEC limit, which will cause a repulsion to excessive majority fermions. This repulsion increases with  $p$ , and may become costly enough so as to render the mean-field superfluid solution unstable. As a result, the distribution of paired fermions is now roughly given by that of the minority fermions,  $n_{\mathbf{k}\downarrow} = \Theta(E_{\mathbf{k}\uparrow})v_{\mathbf{k}}^2$ , which reduces to  $v_{\mathbf{k}}^2$  for  $p = 0$ .

Unlike the  $p = 0$  case, for which hole-like pairing takes place in the weaker coupling regime when  $t$  is small and/or  $d$  is large, here hole-like pairing occurs in the BEC regime via a completely different mechanism. As mentioned above, all the three cases shown in Fig. 7 have a closed noninteracting Fermi surface. As the pairing becomes stronger, the momentum distribution of  $v_{\mathbf{k}}^2$  in the  $xy$  plane extends to the entire first BZ, and becomes roughly a constant at strong coupling; in the absence of population imbalance, this would lead to a rough cancellation (via averaging over the inverse fermion band mass) due to the particle-hole symmetry of the lattice band. However, for any finite  $p$ , the excessive majority fermions will tend to occupy the low  $(k_x, k_y)$  states, and thus expel paired fermions toward higher  $(k_x, k_y)$  states, which have a negative

(i.e., hole-like) band mass, leading to a net hole-like contribution to  $a_0$  in the pair propagator, when integrated over the entire BZ. This also explains why the  $a_0 = 0$  line leans toward weaker coupling with increasing  $p$ .

Shown in Fig. 8 is an example of the momentum distributions of  $v_{\mathbf{k}}^2$  (left),  $n_{\mathbf{k}\downarrow}$  (middle) and  $\delta n_{\mathbf{k}}$  (right column) in the  $(k_x, k_y)$  plane at different  $k_z/k_F = 0$  (top), 0.2 (middle) and 0.4 (bottom row), with  $U/U_c = 4$  and  $p = 0.05$ , for  $t/E_F = 0.15$  and  $k_F d = 1.5$ . This corresponds to a PDW state in Fig. 7(c). Indeed, the excessive fermion distribution,  $\delta n_{\mathbf{k}} = \Theta(-E_{\mathbf{k}\uparrow})$ , occupies the low in-plane momentum part and below  $k_z/k_F = 0.4$  (right column). In addition,  $v_{\mathbf{k}}^2$  (left column) remains roughly constant in the entire BZ and for  $|k_z/k_F| \leq 0.4$ . Most interestingly, the minority fermion distribution  $n_{\mathbf{k}\downarrow}$  (middle column) is given by  $v_{\mathbf{k}}^2$  but with a hole dug out at the center, due to the Pauli repulsion with the excessive fermions.

As a representative example, we show in Fig. 5 the behavior of (a)  $\mu_\sigma$  and (b) the gap  $\Delta$  for  $p = 0.05$  (red) and 0.1 (blue) with fixed  $t/E_F = 0.05$  and  $k_F d = 1$ , as a function of  $U$ . They correspond to horizontal cuts at  $p = 0.05$  and

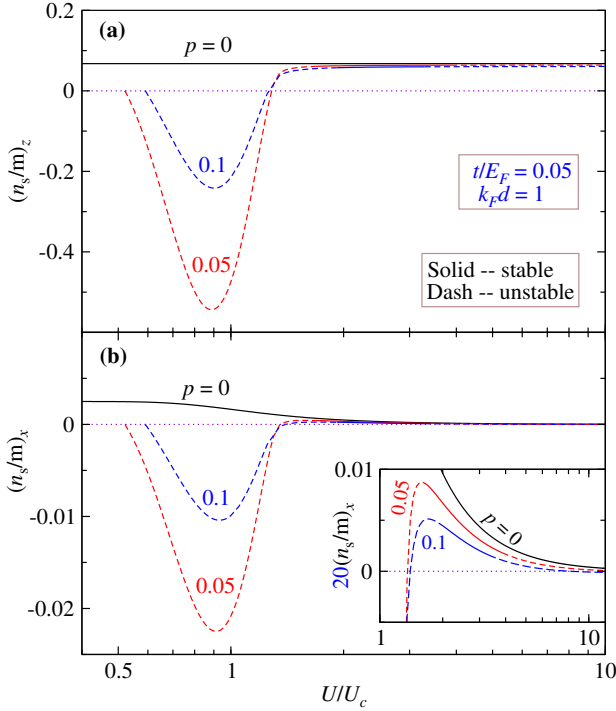


Figure 9. Superfluid density (a)  $(n_s/m)_z$  and (b)  $(n_s/m)_x$  as a function of  $U/U_c$  for  $p = 0$  (black), 0.05 (red) and 0.1 (blue) at  $t/E_F = 0.05$  and  $k_F d = 1$ . Solid (dashed) lines denote stable (unstable) solutions. Shown in the inset is 20 times magnified  $(n_s/m)_x$  vs  $U/U_c$ .

0.1 in Fig. 7(b), and should be compared with the  $p = 0$  case (black solid curves). The solid part of these lines are stable pSF solutions, while the dashed lines are unstable mean-field solutions. There are a few remarkable features. Firstly, the excitation gap changes only slowly with imbalance  $p$ , except that it does not have a solution below certain threshold of interaction strength. Secondly, at given pairing strength,  $\mu_\sigma$  for  $p = 0.05$  and  $p = 0.1$  are very close to each other, but both far separated from the  $\mu$  curve for  $p = 0$ . This again indicates that the  $p \rightarrow 0^+$  case is not continuously connected to the  $p = 0$  case; with a tiny bit of imbalance,  $\mu_\uparrow$  and  $\mu_\downarrow$  immediately split up. Lastly,  $\mu_\uparrow$  increases slowly with pairing strength in the BEC regime. This is different from its counterpart in 3D continuum and 1DOL; for the former,  $\mu_\uparrow$  decreases while for the latter  $\mu_\uparrow$  approaches a  $p$ -dependent constant asymptote, as the pairing strength increases toward the BEC limit. This can be attributed to the emergence of hole-like pairing (with  $a_0 < 0$ ) in the strong pairing regime as the number of lattice dimensions increases. To verify this idea, we have also checked the mean-field solution for imbalanced 3DOL, and found that, indeed,  $\mu_\uparrow$  also increases with the pairing strength in the BEC regime at  $T = 0$ , along with a negative  $a_0$ .

Finally, we present the typical behavior of the superfluid density in the imbalanced case. Shown in Fig. 9 are (a)  $(n_s/m)_z$  and (b)  $(n_s/m)_x$  in the continuum and lattice dimensions, respectively, as a function of  $U/U_c$  for  $p = 0$ , 0.05 and 0.1 at fixed  $t/E_F = 0.05$  and  $k_F d = 1$ . Here solid and

dashed lines are stable and unstable solutions, respectively. As expected, both are always positive for the balanced case. In addition,  $(n_s/m)_x$  is much smaller than  $(n_s/m)_z$ , because it involves the average of the inverse band mass. For the imbalanced case, the superfluid density deviates continuously from its positive  $p = 0$  value as  $p$  increases from 0. However, in the unitary and weak coupling regimes, both continuum and lattice components will become negative for  $p \neq 0$ . Furthermore, the superfluid density is more negative for smaller (but finite)  $p$ . This implies an immediate discontinuous jump from the  $p = 0$  value to a large negative value for  $p = 0^+$  in this regime. Note that for strong enough interaction,  $(n_s/m)_x$  will again change sign to negative, but gradually rather than abruptly, as can already be seen from the  $p = 0.1$  curve. This has to do with the lattice induced confinement in the momentum space and the Pauli exclusion between paired and excessive fermions.

So far, it is not yet clear whether the PDW state can sustain a superfluid order, with and without an imbalance. If the answer is yes, then it will become a supersolid state rather than a Cooper pair insulator. We leave this to a future study.

It should be noted that we have worked with a system with homogeneous fixed densities. For this reason, we have not chosen to use  $\mu$  and  $h$  as control variables, which are more appropriate for systems connected with a large reservoir so that the chemical potentials are fixed or can be tuned separately. In such a case, all  $h < \sqrt{\min(0, \mu)^2 + \Delta^2}$  corresponds to the population balanced state. One can, however, convert between these two approaches, by calculating corresponding densities (and Fermi energy) for given  $\mu$  and  $h$ , and performing a rescaling.

#### IV. CONCLUSIONS

In summary, we have studied the superfluid phase diagram of Fermi gases with a short range pairing interaction in 2DOL at zero temperature with and without population imbalance in the context of BCS-BEC crossover. We find that the mixing of lattice and continuum dimensions, together with population imbalance, has an extraordinary effect on pairing and the superfluidity of atomic Fermi gases. For the balanced case, the ground state is a stable superfluid, except that a PDW ground state emerges for a finite range of intermediate pairing strength in the case of relatively small  $t$  and large  $d$ , and the nature of the in-plane and overall pairing may change from particle-like to hole-like in the BCS and unitary regimes for these  $t$  and  $d$ , which are associated with an open Fermi surface on the BZ boundary of the lattice dimensions. Thus the phase space for the PDW ground state and hole-like pairing shrinks with increasing  $t$  and/or decreasing  $d$ .

For the imbalanced case, the presence of population imbalance has a dramatic detrimental effect, in that the stable polarized superfluid phase occupies only a small region in the bosonic regime in the multi-dimensional phase space, and will shrink and disappear with increasing  $d$  and  $p$  and decreasing  $t$ . The pSF phase can be found only for relatively large  $t$  and small  $d$ , associated with a closed non-interacting Fermi sur-

face, as well as for low  $p$ . In comparison with 3D continuum, the presence of lattice dimensions introduces confinement in the momentum space, which leads to strong Pauli repulsion between paired and excessive fermions. Due to this repulsion, the nature of pairing changes from particle-like to hole-like in the strong pairing regime, and a PDW phase emerges next to the pSF phase. In addition to the normal gas phase, stability analysis shows that an unstable mean-field solution exists and may yield to phase separation (and possibly FFLO) in the rest of the phase diagram. These findings for 2DOL are very different from pure 3D continuum, 3D lattices, and 1DOL, and

should be tested in future experiment.

## V. ACKNOWLEDGMENTS

This work was supported by the National Natural Science Foundation of China (Grant No. 11774309), the Innovation Program for Quantum Science and Technology (Grant No. 2021ZD0301904), as well as the University of Science and Technology of China.

- 
- [1] Q. J. Chen, J. Stajic, S. N. Tan, and K. Levin, BCS–BEC crossover: From high temperature superconductors to ultracold superfluids, *Phys. Rep.* **412**, 1 (2005).
  - [2] I. Bloch, J. Dalibard, and W. Zwerger, Many-body physics with ultracold gases, *Rev. Mod. Phys.* **80**, 885 (2008).
  - [3] C. Chin, R. Grimm, P. Julienne, and E. Tiesinga, Feshbach resonances in ultracold gases, *Rev. Mod. Phys.* **82**, 1225 (2010).
  - [4] M. W. Zwierlein, A. Schirotzek, C. H. Schunck, and W. Ketterle, Fermionic superfluidity with imbalanced spin populations, *Science* **311**, 492 (2006).
  - [5] G. B. Partridge, W. Li, R. I. Kamar, Y.-a. Liao, and R. G. Hulet, Pairing and phase separation in a polarized Fermi gas, *Science* **311**, 503 (2006).
  - [6] M. M. Forbes, E. Gubankova, W. V. Liu, and F. Wilczek, Stability Criteria for Breached-Pair Superfluidity, *Physical Review Letters* **94**, 017001 (2005).
  - [7] C.-H. Pao, S.-T. Wu, and S.-K. Yip, Superfluid stability in the BEC-BCS crossover, *Physical Review B* **73**, 132506 (2006).
  - [8] W. Yi and L.-M. Duan, Trapped fermions across a Feshbach resonance with population imbalance, *Physical Review A* **73**, 031604(R) (2006).
  - [9] Q. J. Chen, Y. He, C.-C. Chien, and K. Levin, Stability conditions and phase diagrams for two-component Fermi gases with population imbalance, *Physical Review A* **74**, 063603 (2006).
  - [10] T. N. De Silva and E. J. Mueller, Profiles of near-resonant population-imbalanced trapped Fermi gases, *Physical Review A* **73**, 051602(R) (2006).
  - [11] M. Haque and H. T. C. Stoof, Pairing of a trapped resonantly interacting fermion mixture with unequal spin populations, *Physical Review A* **74**, 011602(R) (2006).
  - [12] L. Radzihovsky and D. E. Sheehy, Imbalanced Feshbach-resonant Fermi gases, *Reports on Progress in Physics* **73**, 076501 (2010).
  - [13] K. Martiyanov, V. Makhalov, and A. Turlapov, Observation of a two-dimensional Fermi gas of atoms, *Physical Review Letters* **105**, 030404 (2010).
  - [14] C.-T. Wu, B. M. Anderson, R. Boyack, and K. Levin, Quasi-condensation in two-dimensional Fermi gases, *Physical review letters* **115**, 240401 (2015).
  - [15] L. F. Zhang, Y. M. Che, J. B. Wang, and Q. J. Chen, Exotic superfluidity and pairing phenomena in atomic Fermi gases in mixed dimensions, *Scientific reports* **7**, 1 (2017).
  - [16] I. Bloch, Ultracold quantum gases in optical lattices, *Nat. Phys.* **1**, 23 (2005).
  - [17] M. Köhl, H. Moritz, T. Stöferle, K. Günter, and T. Esslinger, Fermionic atoms in a three dimensional optical lattice: Observing Fermi surfaces, dynamics, and interactions, *Physical Review Letters* **94**, 080403 (2005).
  - [18] U. Schneider, L. Hackermüller, S. Will, T. Best, I. Bloch, T. A. Costi, R. Helmes, D. Rasch, and A. Rosch, Metallic and insulating phases of repulsively interacting fermions in a 3D optical lattice, *Science* **322**, 1520 (2008).
  - [19] C.-C. Chien, Q. J. Chen, Y. He, and K. Levin, Intermediate-temperature superfluidity in an atomic Fermi gas with population imbalance, *Physical Review Letters* **97**, 090402 (2006).
  - [20] P. Nozières and S. Schmitt-Rink, Bose condensation in an attractive fermion gas: from weak to strong coupling superconductivity, *J. Low Temp. Phys.* **59**, 195 (1985).
  - [21] Q. J. Chen, I. Kosztin, B. Jankó, and K. Levin, Superconducting transitions from the pseudogap state:  $d$ -wave symmetry, lattice, and low-dimensional effects, *Physical Review B* **59**, 7083 (1999).
  - [22] V. L. Berezinskii, Destruction of long-range order in one dimensional and two dimensional systems possessing a continuous symmetry group II. Quantum systems, *Sov. Phys. JETP* **34**, 610 (1972), *zh. Eksp. Teor. Fiz.* **61**(3), 1144-1156 (1971); J. M. Kosterlitz and D. J. Thouless, Ordering, metastability and phase transitions in two dimensional systems, *J. Phys. C: Solid State* **6**, 1181 (1973).
  - [23] A. T. Sommer, L. W. Cheuk, M. J. H. Ku, W. S. Bakr, and M. W. Zwierlein, Evolution of Fermion Pairing from Three to Two Dimensions, *Physical Review Letters* **108**, 045302 (2012).
  - [24] Y.-a. Liao, A. S. C. Rittner, T. Paprotta, W. Li, G. B. Partridge, R. G. Hulet, S. K. Baur, and E. J. Mueller, Spin-imbalance in a one-dimensional Fermi gas, *Nature* **467**, 567 (2010).
  - [25] G. Pagano, M. Mancini, G. Cappellini, P. Lombardi, F. Schäfer, H. Hu, X.-J. Liu, J. Catani, C. Sias, M. Inguscio, *et al.*, A one-dimensional liquid of fermions with tunable spin, *Nat. Phys.* **10**, 198 (2014).
  - [26] M. C. Revelle, J. A. Fry, B. A. Olsen, and R. G. Hulet, 1D to 3D crossover of a spin-imbalanced Fermi gas, *Phys. Rev. Lett.* **117**, 235301 (2016).
  - [27] C. Cheng, J. Kangara, I. Arakelyan, and J. E. Thomas, Fermi gases in the two-dimensional to quasi-two-dimensional crossover, *Phys. Rev. A* **94**, 031606(R) (2016).
  - [28] L. Sobirey, H. Biss, N. Luick, M. Bohlen, H. Moritz, and T. Lompe, Comparing fermionic superfluids in two and three dimensions, (2021), arXiv:2106.11893.
  - [29] M. G. Ries, A. N. Wenz, G. Zürn, L. Bayha, I. Boettcher, D. Kedar, P. A. Murthy, M. Neidig, T. Lompe, and S. Jochim, Observation of Pair Condensation in the Quasi-2D BEC-BCS Crossover, *Physical Review Letters* **114**, 230401 (2015).
  - [30] P. A. Murthy, I. Boettcher, L. Bayha, M. Holzmann, D. Kedar, M. Neidig, M. G. Ries, A. N. Wenz, G. Zürn, and S. Jochim, Observation of the Berezinskii-Kosterlitz-Thouless Phase Transition in an Ultracold Fermi Gas, *Physical Review Letters* **115**,

- 010401 (2015).
- [31] D. Mitra, P. T. Brown, P. Schauß, S. S. Kondov, and W. S. Bakr, Phase Separation and Pair Condensation in a Spin-Imbalanced 2D Fermi Gas, *Physical Review Letters* **117**, 093601 (2016).
  - [32] B. C. Mulkerin, L. He, P. Dyke, C. Vale, X.-J. Liu, and H. Hu, Superfluid density and critical velocity near the Berezinskii-Kosterlitz-Thouless transition in a 2d strongly interacting Fermi gas, *Phys. Rev. A* **96**, 053608 (2017).
  - [33] K. Hueck, N. Luick, L. Sobirey, J. Siegl, T. Lompe, and H. Moritz, Two-Dimensional Homogeneous Fermi Gases, *Phys. Rev. Lett.* **120**, 060402 (2018).
  - [34] J. B. Wang, L. Sun, Q. Zhang, L. F. Zhang, Y. Yu, C. H. Lee, and Q. J. Chen, Superfluidity and pairing phenomena in ultracold atomic Fermi gases in one-dimensional optical lattices. II. Effects of population imbalance, *Physical Review A* **101**, 053618 (2020).
  - [35] L. Sun, J. B. Wang, X. Chu, and Q. J. Chen, Pairing phenomena and superfluidity of atomic Fermi gases in a two-dimensional optical lattice: Unusual effects of lattice-continuum mixing, *Annalen der Physik* **534**, 2100511 (2022).
  - [36] A. J. Leggett, Diatomic molecules and cooper pairs, in *Modern trends in the theory of condensed matter* (Springer, 1980) pp. 13–27.
  - [37] Y. M. Che, J. B. Wang, and Q. J. Chen, Reentrant superfluidity and pair density wave in single-component dipolar Fermi gases, *Phys. Rev. A* **93**, 063611 (2016).
  - [38] J. B. Wang, L. F. Zhang, Y. Yu, C. H. Lee, and Q. J. Chen, Superfluidity and pairing phenomena in ultracold atomic Fermi gases in one-dimensional optical lattices. I. Balanced case, *Phys. Rev. A* **101**, 053617 (2020).
  - [39] L. F. Zhang, J. B. Wang, Y. Yu, and Q. J. Chen, Ultra high temperature superfluidity in ultracold atomic Fermi gases with mixed dimensionality, *Sci. China - Phys. Mech. Astron.* **63**, 227421 (2020).
  - [40] Q. J. Chen, I. Kosztin, B. Jankó, and K. Levin, Pairing fluctuation theory of superconducting properties in underdoped to overdoped cuprates, *Phys. Rev. Lett.* **81**, 4708 (1998).
  - [41] For the latter case, one can perform a particle-hole transformation so that it becomes  $a_0 > 0$  and below half filling for holes.
  - [42] Q. J. Chen, J. B. Wang, L. Sun, and Y. Yu, Unusual Destruction and Enhancement of Superfluidity of Atomic Fermi Gases by Population Imbalance in a One-Dimensional Optical Lattice, *Chinese Physics Letters* **37**, 053702 (2020).
  - [43] C.-H. Pao, S.-T. Wu, and S.-K. Yip, Superfluid stability in the bec-bcs crossover, *Physical Review B* **73**, 132506 (2006).
  - [44] Y. He, C.-C. Chien, Q. J. Chen, and K. Levin, Thermodynamics and superfluid density in bcs-bec crossover with and without population imbalance, *Physical Review B* **76**, 224516 (2007).
  - [45] Q. J. Chen, *Generalization of BCS theory to short coherence length superconductors: A BCS-Bose-Einstein crossover scenario*, Ph.D. thesis, University of Chicago (2000), available as arXiv:1801.06266.
  - [46] Q. J. Chen, Y. He, C.-C. Chien, and K. Levin, Theory of superfluids with population imbalance: Finite-temperature and bcs-bec crossover effects, *Physical Review B* **75**, 014521 (2007).
  - [47] C.-C. Chien, Y. He, Q. J. Chen, and K. Levin, Superfluid-insulator transitions at noninteger filling in optical lattices of fermionic atoms, *Phys. Rev. A* **77**, 011601(R) (2008).
  - [48] C.-C. Chien, Q. J. Chen, and K. Levin, Fermions with attractive interactions on optical lattices and implications for correlated systems, *Phys. Rev. A* **78**, 043612 (2008).
  - [49] P. Fulde and R. A. Ferrell, Superconductivity in a strong spin-exchange field, *Phys. Rev.* **135**, A550 (1964); A. I. Larkin and Y. N. Ovchinnikov, Inhomogeneous state of superconductors, *Sov. Phys. JETP* **20**, 762 (1965), [*Zh. Eksp. Teor. Fiz.* **47**, 1136 (1964)].
  - [50] J. B. Wang, Y. M. Che, L. F. Zhang, and Q. J. Chen, Instability of Fulde-Ferrell-Larkin-Ovchinnikov states in three and two dimensions, *Phys. Rev. B* **97**, 134513 (2018).
  - [51] K. V. Samokhin and M. S. Mar'enko, Quantum fluctuations in larkin-ovchinnikov-fulde-ferrell superconductors, *Phys. Rev. B* **73**, 144502 (2006).
  - [52] A. Cichy and R. Micnas, The spin-imbalanced attractive Hubbard model in  $d=3$ : Phase diagrams and BCS-BEC crossover at low filling, *Ann. Phys.* **347**, 207 (2014).